Root responses to different types of TiO2 nanoparticles and bulk counterpart in plant model system Vicia faba L.

Root responses to different types of TiO_2 nanoparticles and bulk counterpart in plant model system *Vicia faba* L.

Monica Ruffini Castiglione[1*], Lucia Giorgetti[2], Lorenza Bellani[2,3], Simonetta Muccifora[3], Stefania Bottega[1], Carmelina Spanò[1]

[1]Department of Biology, University of Pisa, Via Ghini 13, 56126 Pisa, Italy; [2]Institute of Agricultural Biology and Biotechnology, UOS Pisa, CNR, Via Moruzzi 1, 56124 Pisa, Italy; [3]Department of Life Sciences, University of Siena, Via A. Moro 2, 53100 Siena, Italy

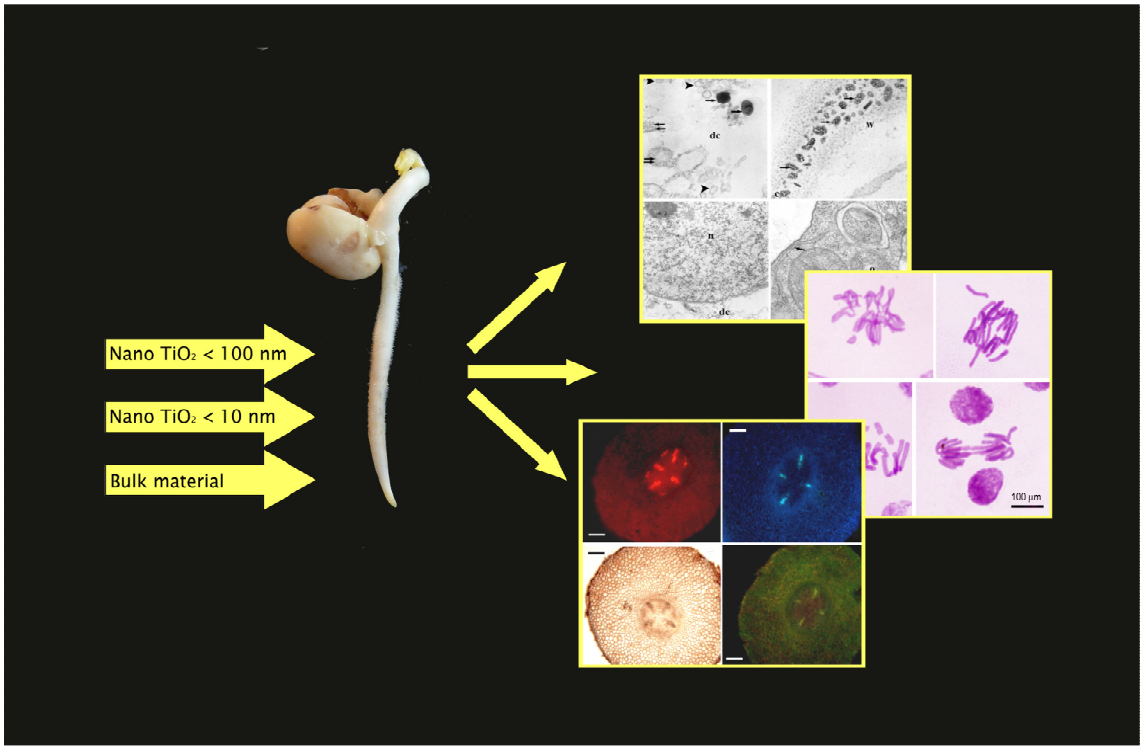

*Corresponding author: monica.ruffini.castiglione@unipi.it, tel. +390502211317

All the authors contributed equally to the article

Abstract

The aim of the present work was to study , in the model system *Vicia faba* L., the potential stress-induced response to a commercial source of TiO_2 nanoparticles (NPs) <100nm (tetragonal crystals), to a TiO_2-NPs laboratory-made sample <10nm (spherical shape), and to the corresponding bulk material, recently classified as possibly carcinogenic to humans.

The above materials were applied to *V. faba* seeds up to early seedling development; different endpoints were considered to estimate possible phytotoxic and genotoxic effects at ultrastructural, cyto-histological and physiological level. Oxidative stress and antioxidant response were evaluated by biochemical approach and *in situ* histochemical techniques. Ultrastructural studies demonstrated that the applied NPs were internalized in root plant cells but the most damages to the cellular appearance followed bulk material treatment. Our results on seed vigor index, on aberration index, on the evaluation of oxidative stress and of induced antioxidant response demonstrated that TiO_2-NPs may exert specific actions at different levels of toxicity, depending on their size and shape and that the bulk counterpart seems to provoke the major adverse effects in *V. faba* root.

Keywords: bulk material, faba bean, genotoxicity, oxidative stress, titanium dioxide nanoparticles, ultrastructural studies

1. Introduction

Nanotechnologies are a tremendous opportunity for their positive impact in many sectors of economy, in industrial applications and in scientific research, but with unavoidable environmental emission and release of new chemicals. Nanoparticles (NPs) find their way into aquatic, terrestrial and atmosphere environments, where their fate and behaviour depend on the particle type, on their aggregation tendency and on bioavailability (Hotze et al., 2010). Therefore plants, organisms that strongly interact with their immediate environment, are expected to be affected by their exposition to NPs. As a consequence NPs have been recently included among the emerging contaminants by USEPA (2010). From the first decade of two thousand the first papers published on the potential effects of NPs on higher plants (Ma et al., 2010; Navarro et al., 2008; Ruffini Castiglione and Cremonini, 2009) evidenced some crucial points:

a) NPs, strongly enhancing or modifying the properties of the bulk materials, can interact in a non-predictable way with the environment and the living organisms;

b) NPs can explicate their actions depending on both the chemical composition and on the size and/or shape of the particles themselves;

c) NPs effects depend on the plant organism considered and on the variety of endpoints employed, sometimes making difficult comparative studies. In addition, the evaluation of specific effects, although fundamental to the understanding of the toxicity mechanisms, cannot be extended to all plant systems.

In the light of these considerations we can emphasize that the studies conducted so far on the phytotoxicity of NPs have produced data inadequate to characterize unambiguously their actions on plants, although many results demonstrate effects on *in vitro* cell culture,

64 embryogenesis, growth, biochemical processes and gene expression (Giorgetti et al., 2011;
65 Kaveh et al., 2013; Poborilova et al., 2013).
66 TiO_2-NPs, for their high stability, anticorrosive properties, redox selectivity, low production
67 costs and their wide spectrum of new applications, are among the top five NPs used in
68 consumer products (Chuankrerkkul and Sangsuk, 2008). Most of NPs applications are related
69 to their characteristics of white pigment, four million tons being consumed annually
70 worldwide (Ortlieb, 2010). Furthermore TiO_2-NPs are widely used in common products
71 (toothpastes, sunscreens, cosmetics, food products), in specific fields of medicines and
72 pharmaceuticals, in certain sectors of agriculture and in environmental cleanup technologies
73 (Bhawana and Fulekar, 2012; Liu, 2011).
74 Previous studies evidenced both positive and negative effects of TiO_2-NPs on plants. Part
75 of the scientific literature reports their significant improvement of germination, of shoot and
76 root growth, of chlorophyll content, of transpiration and of water use efficiency (Raliya et al.,
77 2015; Seeger et al., 2009; Song et al., 2013; Zheng et al., 2005). On the contrary, other papers
78 report that plants can be harmed by TiO_2-NPs with decrease in biomass, delayed germination,
79 influence on mitotic index and genotoxic effects (Du et al., 2011; Ruffini Castiglione et al.,
80 2011), DNA fragmentation, reactive oxygen species (ROS) production (Ghosh et al., 2010;
81 Ruffini Castiglione et al., 2014) and changes in micro-RNA expression (Frazier et al., 2014).
82 The experimental design of this work was scheduled to study the potential effects of TiO_2-
83 NPs in the model system *Vicia faba*, at 72 h of seed germination, the most widely used
84 treatment time assessing chemical-induced acute adverse effects (Baderna et al., 2015).
85 We choosed a middle-low exposure concentration that possibly might reproduce an actual
86 environmental exposure, estimated by recent probabilistic material-flow modelling studies
87 (Praetorius et al., 2012). On the basis of previous data showing negative effects only induced
88 by high TiO_2 NPs concentrations (Ruffini Castiglione et al., 2014), we hypothesized plant

89 responses, not necessarily associated to toxic effects.

90 We employed two types of TiO_2-NPs to assess if different responses in function of
91 different particle size and characteristics were elicited. In addition, as corresponding bulk
92 material, considered for decades an inert and safe material has been recently classified as
93 possibly carcinogenic to humans (Group 2B carcinogen, IARC 2010), we tested also the
94 effects of the same concentration of this form. To evaluate the hypothesized effects of these
95 materials on *V. faba* seeds, we considered different cytological, physiological, histochemical
96 and biochemical endpoints**.** Given that NPs can influence plant growth and development
97 directly entering plant cells by means of different penetration mechanisms (Chichiriccò and
98 Poma, 2015) or even without being internalized, a further aim of our work was to understand
99 how these materials can affect *V. faba* root ultrastructure in function of the shape and of the
100 size of the NPs.

101

102 **2. Materials and methods**

103 *2.1. Seed germination and seedling development*

104 Seeds of *Vicia faba* L. var. *minor* were washed over night in tap water, germinated at 24±1
105 °C for 72 h in the dark in Petri dishes in water (control, sample C), in a suspension of two
106 rutile/anatase TiO_2-NPs: < 100 nm (sample S: tetragonal crystals, from Sigma-Aldrich, USA);
107 < 10 nm (sample P: spherical shape, produced by pulsed laser ablation in liquids) (Giorgetti et
108 al., 2014), kindly provided by PlasmaTech, Pisa (Italy) and in bulk TiO_2 (sample B, from
109 Sigma-Aldrich, USA). All the treatments were performed at the selected concentration of 50
110 mg/L. For all treatments 5 Petri dishes with 10 seeds each were set up. Three days after
111 treatment, the germination percentage and the seedling root length were evaluated in all
112 samples.

113 Vigour index (VI) was calculated with the following formula:

VI = Germination (%) x Seedling Growth (mm).

Roots were collected for cytological, histochemical and biochemical determinations as described below.

2.2. Transmission electron microscope (TEM)

To evaluate morphology and size of the different TiO_2-NPs, a drop (10 µL, 50 mg/L) of samples S and P was placed on TEM grids covered with formvar, allowed to settle and dry.

For TEM root observations, small cubes of control and treated roots were pre-fixed in Karnovsky solution (Karnovsky, 1965), post-fixed in osmium tetroxide, dehydrated and embedded in Epon 812-Araldite A/M mixture. Thin sections were stained with uranyl acetate and lead citrate.

Isolated NPs and root sections were observed under a FEI Tecnai G2 Spirit electron microscope at 100 kv.

2.3. Cytological studies on root meristem

Ten roots for each treatment were fixed in ethanol: glacial acetic acid (3:1 v/v) for 12 h. Root tips were squashed and stained following Feulgen technique (Giorgetti and Ruffini Castiglione, 2016).

At least 1000 nuclei, randomly selected for each slide, were analyzed by light microscope.

Perturbations in mitotic activity (mitotic index, MI, = number of mitosis/100 nuclei) indicate cytotoxicity, while both micronuclei presence (MNC=Micronucleus frequency/1000 nuclei) and mitotic aberrations (aberration index, AI, = number of aberrations/100 nuclei) indicate the genotoxicity of a treatment. The scored aberrations included chromosomal bridges, fragments, lagging chromosomes, stickiness, aberrant metaphases and disturbed anaphases in dividing cells, micronuclei in interphase cells (Ruffini Castiglione et al., 2011).

139 *2.4. Histochemical detection of oxidative stress on root system*

140 Five roots for each treatment were hand sectioned in correspondence to the initial root hair
141 area. Cross sections were immediately processed with specific staining reagents for
142 fluorescence and optical microscopy. Fluorescence microscope analysis was carried out with a
143 Leica DMLB, equipped with appropriate set of excitation/emission filters and with a Leica
144 DC300 ccd camera; optical microscope analysis was performed with a Leitz Diaplan,
145 equipped with a Leica DCF420 ccd camera. Fluorescent Amplex Ultrared® (Life
146 Technologies, USA) was applied for *in situ* detection of hydrogen peroxide (H_2O_2) following
147 manufacturing instructions. In brief, sections were incubated for 30 min at room temperature
148 (RT) in the dark in the staining mixture composed by 50 µl of 10mM Amplex Ultrared stock
149 solution in DMSO, 100 µl horseradish peroxidase (Sigma-Aldrich, USA) (10 U/ml in 0.05M
150 PB, pH 6), 4.85 ml of 0.05M PB pH 6. After three washes in the same buffer, the slices were
151 mounted in glycerol and observed with fluorescence microscope ($568_{ex}/681_{em}$ nm). Reactive
152 nitrogen species (RNS) were revealed by 2,3-Diaminonaphthalene staining (Life
153 Technologies, USA) dissolved in DMSO (0.5M) and then diluted 1:1000 in PBS 0.05M pH
154 6.8 just before the sample incubation in the dark at RT. After 30 min and three washes in the
155 same buffer, slices were mounted in glycerol for the observations with fluorescence
156 microscope ($365_{ex}/415_{em}$ nm). BODIPY® 581/591 C11 was used as free radical sensor to
157 visualize lipid peroxidation levels as a change of the fluorescence emission peak from red to
158 green. The slices were incubated in 10 µM BODIPY in PBS 0.1M pH 7.4 for 30 min at RT in
159 the dark and then washed three times in the same buffer. Microscope evaluation was
160 performed acquiring simultaneously the green ($485_{ex}/510_{em}$ nm) and the red fluorescence
161 ($581_{ex}/591_{em}$ nm) signals and merging the two images (Kováčik et al., 2014). Endogenous
162 peroxidase activity was visualized under optical microscope exploiting a solution of
163 colourless guaiacol/H_2O_2 (5mM H_20_2, 5mM guaiacol in 60mM PB pH 6.1) that became

dark/brown tetraguaiacol, due to peroxidase activity. After 10 min of incubation the slices were washed three times in the same buffer and mounted in glycerol for microscope analysis (Lepeduš et al., 2005).

2.5. Determination of water content (WC) and of relative water content (RWC)

Fresh weight (FW) was obtained by weighing the fresh roots. The roots were then immersed in water overnight (turgid weight, TW), oven-dried at 100°C to constant weight and reweighed (dry weight, DW).

WC percentage was estimated on the FW basis. RWC was determined as in Balestri et al. (2014) and calculated with the formula:

RWC = [(FW-DW)/(TW-DW)] x 100

2.6. Extraction and determination of H_2O_2 and thiobarbituric acid reactive substances (TBARS)

H_2O_2 content of roots was determined according to Jana and Choudhuri (1982). Roots were ground and homogenised with phosphate buffer 50mM pH 6.5. The homogenate was centrifuged at 6000*g* for 25 min. H_2O_2 content was determined using 0.1% titanium chloride in 20% (v/v) H_2SO_4. The amount of H_2O_2 was detected spectrophotometrically (410 nm), calculated from a standard curve and expressed as µmol g^{-1}DW.

Lipid peroxidation in roots was measured determining the amount of TBARS by the thiobarbituric acid (TBA) reaction (Hartley-Whitaker et al., 2001) with minor modifications. Roots were mixed with TBA reagent (10% w/v trichloroacetic acid + 0.25% w/v thiobarbituric acid), heated (95°C for 30 min), cooled for 15 min and centrifuged at 2000*g* for 15 min. The level of TBARS was detected as specific absorbance at 532 nm by subtracting the non-specific absorbance at 600 nm and calculated using an extinction

coefficient of 155mM^{-1} cm^{-1}. TBARS were expressed in nmol g^{-1} DW.

2.7. Extraction and determination of proline

Proline concentration was determined according to Bates (1973) with minor modifications (Spanò et al., 2013). Root were homogenised with 3% sulfosalicylic acid. The supernatant was incubated with glacial acetic acid and ninhydrin reagent (1:1:1) and boiled at 100°C for 60 min. After cooling the reaction mixture, toluene was added and the absorbance of toluene phase was read at 520 nm. Calculations were made on the base of a standard curve and content was expressed as µmol g^{-1}DW.

2.8. Extraction and determination of ascorbate and glutathione

Ascorbate, reduced form (ASA) and oxidised form (dehydroascorbate, DHA), extraction and determination were performed according to Spanò et al. (2011). Calculations were made on the base of a standard curve. A blank was made in the absence of the extract and content was expressed as µmol g^{-1}DW.

Glutathione was extracted and determined according to Gossett et al. (1994). Total glutathione (reduced form, GSH + oxidised form, GSSG) was detected monitoring the rate of change in absorbance at 412 nm. GSSG was determined after removal of GSH from the extract by 2-vinylpyridine derivatization. GSH was detected by subtracting the amount of GSSG from total glutathione and calculations were made on the base of a standard curve. A blank was made in the absence of the extract and content was expressed as µmol g^{-1}DW.

2.9. Enzyme extraction and assays

Roots were ground in liquid nitrogen and the extraction was made at 4°C as in Spanò et al. (2013). The homogenate was then centrifuged at 15000*g* for 20 min. For ascorbate

214 peroxidase, 2mM ascorbate was added to the extraction medium. Supernatants were
215 collected and stored in liquid nitrogen until their use for enzymatic assays.
216 Ascorbate peroxidase (APX, EC 1.11.1.11) activity was measured according to Nakano
217 & Asada (1981). Enzyme activity was assayed from the decrease in absorbance at 290 nm
218 (extinction coefficient $2.8 mM^{-1}cm^{-1}$) as ascorbate was oxidised and enzyme extract
219 contained 25 µg protein ml^{-1}. Correction was made for the low, non-enzymatic oxidation of
220 ascorbate by H_2O_2 (blank).
221 Glutathione peroxidase (GPX, EC 1.11.1.9) activity was determined according to
222 Navari-Izzo et al. (1997) following the oxidation of NADPH at 340 nm (extinction
223 coefficient 6.2 mm^{-1} cm^{-1}). Enzymatic extract contained 12.5 µg protein ml^{-1}.
224 Catalase (CAT, EC 1.11.1.6) activity was determined according to Aebi (1984).
225 Enzymatic extract contained 12.5 µg protein ml^{-1}. A blank containing only the enzymatic
226 solution was made. Specific activity was calculated from the $39.4 mM^{-1}$ cm^{-1} extinction
227 coefficient.
228 Guaiacol peroxidase (POD, EC 1.11.1.7) activity was determined according to Arezky
229 et al. (2001) using 1% guaiacol as substrate. Enzymatic extract contained 5 µg protein ml^{-1}.
230 Enzymatic activity was determined following guaiacol oxidation by H_2O_2 (extinction
231 coefficient $26.6 mM^{-1}$ cm^{-1}) at 470 nm, one unit oxidising 1.0 µmole guaiacol per min.
232 All enzymatic activities were determined at 25°C and expressed as U g^{-1} protein. Protein
233 measurement was performed according to Bradford (1976), using BSA as standard.
234
235 *2.10. Statistical analysis*
236 All the data were the mean of at least three replicates from three independent experiments.
237 Statistical significance was determined by ANOVA tests followed by *post hoc* Bonferroni
238 multiple comparison test. *Post hoc* statistical significance is indicated in figures and tables

239 by different letters.

240

241 **3. Results**

242 *3.1. Germination and growth*

243 Germination percentage (Table 1) did not show significant differences between control
244 and treated materials. After 72 h germination roots from B treated seeds were significantly
245 shorter than P-NPs treated roots but not significantly different from C and S-NPs treated
246 materials (Fig. 1, Table 1). The highest VI (Table 1) was detected in P-NPs treated roots,
247 while the minimum value was characteristic of B treated samples.

248

249 *3.2. TEM observations*

250 The morphology of the TiO_2 P and S-NPs is shown in Figs 2a and 2b, respectively. Both
251 were extremely variable in electron density (Figs 2a, b). P-NPs were roughly round in shape
252 with a diameter from 2 to 12 nm (Fig. 2a). S-NPs had polyhedral shape and a wide size
253 distribution ranging from 10 to 100 nm (Fig. 2b). Sections of control roots showed cells with
254 large vacuoles with scanty materials evident. The cytoplasm was rich in well structured
255 organelles, particularly long rough endoplasmic reticulum cisternae, dictyosomes,
256 mitochondria and plastids (Fig. 2c). The cell ultrastructure of P-NPs treated roots appeared
257 similar to control ones. The only noteworthy difference was the presence of electron dense
258 particles embedded in scanty electron dense material scattered in the cell vacuole (Fig. 2d).
259 Often dense particles of 5-12 nm were observed crossing the walls of rhizodermis and of root
260 parenchyma cells (Figs 2e, f).

261 The S-NPs treated roots showed cell vacuoles containing single or aggregated NPs (Fig.
262 3a). Several cells showed wide zone of cytoplasmic degeneration (Fig. 3b) often surrounded
263 by a double membrane. In these cytoplasmic portions a large number of small and/or large

vesicles with rough membranes and NPs of polyedric form, isolated or aggregated, were observed (Fig. 3b). Some of these cells showed more or less evident plasmalemma-wall detachment as in plasmolysis (data not shown). In the cell walls of rhizodermis numerous aggregates (60-120 nm) of dense particles were often present (Fig. 3c). Numerous vesicles, smooth endoplasmic reticulum cisternae and organelles, often not well recognizable, were present in the cells of the B treated roots (Fig. 3d). Some cells showed nuclei with extremely disperse chromatin and wide portion of cytoplasmic degeneration (Fig. 3e). Furthermore, a great number of cells evidenced an amazing electron dense cytoplasm with numerous not well recognizable organelles (probably plastids), amyloplasts and weakly electron opaque bodies of about 0.3- 0.5 µm in diameter (Fig. 3f).

3.3. Cytological evaluation of the root meristem

The mitotic activity (MI) and the occurrence of micronuclei in interphase (MNC), evidenced not significant disturbances under different treatments. On the contrary, when the frequency of anomalies and/or aberrations (AI) in dividing cells were recorded, a significant increase in the AI was observed for the samples S and B, while the mean value of the AI in the samples P was not statistically different from the control (Fig. 4). Fig. 5 shows some representatives examples of the scored mitotic abnormalities.

3.4. Histological evaluation associated to in situ detection of oxidative stress

Probes specific for H_2O_2, RNS, lipid peroxidation and guaiacol-peroxidase activity (Fig. 6) directly detect qualitative signals related to oxidative stress. In cross sections of control and treated roots the signal obtained with the fluorescent probe Amplex H_2O_2, apart from a faint staining involving the cortical area, was mainly localized in xylem vessels (Fig. 6a). In the samples treated with both the types of NPs we observed a general increase of H_2O_2 in the

289 vascular cylinder involving as well the phloem, alternated between the arms of the xylem
290 (Figs 6b, c). On the contrary, the roots treated with bulk material showed a strong staining in
291 the rhizodermis and in the periphery of the cortical cylinder (Fig. 6d).
292 Concerning the RNS, the control root presented a distinctive blue staining involving
293 mainly the xylem vessels, and, to a lesser extent, the region surrounding the stele and the
294 peripheral area of the cortex (Fig. 6e). Under treatments, we observed a general increase of
295 the fluorescence intensity in respect to the control, especially in the samples S and B (Figs 6f,
296 g, h). Sample B was the most reactive also at the BODIPY fluorescent probe (Fig. 6l), which
297 identified lipid peroxidation as a change of the fluorescence emission peak from red to green.
298 In this sample the green fluorescence was observed in all the root tissues, with the exception
299 of the central part of the stele. Samples P and S (Figs 6j, k) were similar to the control (Fig.
300 6i) as to the intensity of the staining in the root cortex, but a well defined green area
301 corresponding to the perycicle and to the outermost cells of vascular tissues was observed in
302 sample S (Fig. 6k). Figs 6m-p shows representative sections after guaiacol staining. The
303 brown colour indicates peroxidase activity induced by treatments. Root cross sections were
304 lightly stained in samples C and P (Figs 6m, n), the former showing a more diffuse signal, the
305 latter being more sharply stained, also in the area of phloem arcs. Guaiacol reaction strongly
306 increased in the S and B samples (Figs 6o, p).
307
308 *3.5. Water content and relative water content*
309 Bulk-treated material was characterized by the highest values of both WC and RWC (Table
310 1). Roots of NPs-treated samples, on the other hand, showed all similar hydric status.
311
312 *3.6. H_2O_2 and TBARS*
313 The highest contents of H_2O_2 and TBARS (Table 1) were detected in B roots. H_2O_2

concentration was lower in C roots and even more in S samples, showing the lowest value in P-NPs treated material. Both NPs-treated roots had TBARS content not significantly different from C roots.

3.7. Proline and low molecular weight antioxidants

Proline (Table 1) had the highest value in C roots, was significantly lower in B and even more in NPs-treated seeds, regardless of the type of NPs used. B roots were characterized by the highest contents of both total ascorbate and glutathione (Table 1). P-NPs treated roots showed the lowest values of these low molecular weight antioxidants, while S roots did not differ significantly from control material. Interestingly, the highest values of reducing power of ASA/DHA couples were characteristic of NPs-treated roots. Significantly high was the GSH/GSSG ratio in sample P (Table 1).

3.8. Antioxidant enzymes

Although no significant difference was observed in GPX activity among different treatments, both APX and CAT activities were significantly lower in all treated roots, regardless of the type of treatment (Table 1). The highest POD activity was detected in S-NPs treated roots, significantly lower values in B then in C samples and the lowest activity in P-NPs treated samples.

4. Discussion

NPs can influence plant growth and development without being internalized (Asli and Neumann, 2009) or directly entering plant cells by means of different penetration mechanisms (Chichiriccò and Poma, 2015), also when they have dimensions higher than cell wall pore exclusion limit (Larue et al., 2012). However, few literature data are available concerning the

339 effects of TiO_2-NPs and bulk material on root ultrastucture. The present ultrastructural
340 observations confirmed the presence of TiO_2-NPs inside *V. faba* root cells and provided
341 significant information on their effects. The NPs penetrated through the cell walls of
342 rhizodermis and moved via the apoplast pathway. Indeed they were observed in the P-NPs
343 treated root wall generally as individual particles, while the S-NPs crossed the rhizodermis
344 walls as aggregates. The wall pore size can allow the diffusion of molecules (exceptionally)
345 up to 10 nm of diameter (Larue et al., 2012), as a consequence the P-NPs can cross the
346 rhizodermis and move through the apoplasm. It was supposed a NPs induction of hydroxyl
347 radicals that can loose the wall with enlargement of pores by cleavage of pectin-
348 polysaccharides (Kim et al., 2014; Larue et al., 2012). In this way it is possible to explain the
349 wall penetration of the large particles and of S-NPs aggregates. The vacuolar sequestration of
350 P-NPs allows to avoid interaction of particles with organelles and metabolic process. The
351 success of this detoxification mechanism is attested by the fact that the cell ultrastructure of
352 P-NPs treated roots appeared similar to the control ones. On the contrary, in S-NPs treated
353 roots the NPs were localized both in the vacuoles and in wide zones of degenerated
354 cytoplasm, often surrounded by a double membrane. These findings recall the double
355 membrane autophagosomes that form in response to biotic and abiotic stress and can bring to
356 programmed cell death (Kutik et al., 2014). This process is characterized by gradual lysis of
357 the cellular content leaving at the end the hollow cell wall shell (Kutik et al., 2014).
358 Therefore, in *V. faba* the damage of the cell ultrastructure appeared to be related to size and
359 shape of NPs. B treatment strongly affected cell ultrastructure, as electron dense cytoplasm
360 and numerous not well recognizable organelles (probably plastids), amyloplasts, and weakly
361 electron opaque bodies of about 0.3-0.5 μm diameter were observed, giving the appearance of
362 not yet differentiated embryo cells.

363 Contrasting results were reported about the effects of TiO_2-NPs on plant germination and

364 growth (Ghosh et al., 2010; Ruffini Castiglione et al., 2011, 2014; Seeger et al., 2009; Song et
365 al., 2013). In *V. faba* the different treatments of TiO_2-NPs and bulk material did not cause
366 germination inhibition, but bulk material induced the production of seedlings with the shortest
367 roots. This is in contrast with Azimi et al. (2013) who reported no variation in root length in
368 seeds of *Agropyron desertorum* treated with similar concentrations of bulk TiO_2. Additional
369 interesting information can derive from VI, which, summarizing the impact of a particular
370 compound on seed germination and seedling growth, can give an idea of the whole
371 germination process (Ruffini Castiglione et al., 2014). Our previous data on another species of
372 *Vicia* revealed a phytotoxic effect only at the highest (4‰) S-NPs concentration. In
373 accordance, *V. faba* treated with low concentrations of S-NPs had a VI comparable with that
374 of C material. The increase in VI induced by P-NPs was in accordance with reports by Feizi et
375 al. (2013) for sage underlining a different action of NPs in function of the size and shape.
376 Despite the minor root growth, B-treated plants were characterized by a good hydric status, as
377 indicated by WC and RWC, showing that the impaired root growth was not due to tissue
378 water deficit.

379 DNA injuries and genotoxic effects were demonstrated after TiO_2-NPs treatments both in
380 animal (Shukla et al., 2013) and in plant systems (Ghosh et al., 2010; Ruffini Castiglione et
381 al., 2011, 2014; Moreno-Olivas et al., 2014; Pakrashi et al., 2014) by different experimental
382 approaches such as comet assay, chromosomal aberration analysis, micronuclei assay, γ-
383 H2AX assay, DNA laddering assay and RAPD analysis.

384 Concerning cytological evaluation of the root meristem behaviour, in contrast to what was
385 observed in the root apex following plant treatments with nano- and macroscale metals
386 (Kumari et al., 2009; Balestri et al., 2014), no negative effect was registered for the mitotic
387 activity in our experimental conditions: all the recorded MI were not significantly different
388 from the control, indicating absence of cytotoxicity for all the treatments. Also the MNC,

389 recently standardized for *V. faba* by an international protocol, ISO 29200 (Cotelle et al.,
390 2015), did not reveal toxic effects on root apex. In this plant system, the absence of
391 micronuclei induction occurred in parallel with an increase in the frequency of AI in samples
392 S and B. The lack of concordance between MNC test and AI in these two treatments indicated
393 that S-NPs and the bulk counterpart could act as indirect toxicants and/or exert on
394 meristematic cells a delayed effect along 72 hours of treatment, allowing to detect only
395 anomalies and/or aberrations in dividing cells but not the resulting micronuclei in the
396 subsequent interphase. Genotoxic effects of S-NPs were already observed on *V. narbonensis*
397 and *Zea mays* (Ruffini Castiglione et al., 2011) at higher concentrations (200-4000 mg/L);
398 besides bulk material provoked a genotoxic response in *Allium cepa* at about 100 mg/L and
399 above (Ghosh et al., 2010).
400 The genotoxicity of NPs, supposed to be due to oxidative stress as the primary key
401 mechanism inducing DNA damages, strongly coupled to ROS activity and to depletion of cell
402 antioxidant response. ROS, such as superoxide, H_2O_2 and hydroxyl radicals may act as
403 elicitors of common stress response (Mittler, 2002); however when they accumulate at critical
404 level an oxidative stress can ensue (Parida and Das, 2005). Nevertheless, H_2O_2 may act as an
405 active regulator of biological processes related to growth and differentiation (Bellani et al.,
406 2012), as observed in tracheary elements and in endodermis of the control and all the treated
407 samples.
408 Previous studies showed that NPs can induce both increase (Zhao et al., 2012) and
409 decrease (Sharma et al., 2012) in H_2O_2 content, even in the same species in a NPs
410 concentration-dependent manner (Ruffini Castiglione et al., 2014). In our experimental
411 conditions, in accordance with data on *Cicer arietinum* (Mohammadi et al., 2014), TiO_2-NPs
412 induced a significant decrease in the content of this molecule, the lowest value characterizing
413 P-NPs treated roots. The low H_2O_2 content for P and S-NPs treated materials could be due at

414 least in part to a possible radical scavenging activity of TiO_2-NPs, higher at the decrease in
415 particle size and increase in surface area (Kalyanasundharam and Prakash, 2015). This
416 scavenging role could be very helpful in increasing plant tolerance under stress condition
417 (Mohammadi et al., 2014). Roots treated with P and S-NPs showed a peculiar staining pattern
418 of H_2O_2 in different root compartments, involving mainly the vascular cylinder and the
419 phloem arcs: this H_2O_2 localization may be allied to a different root response elicited by the
420 nanomaterials. The highest content of H_2O_2 was detected in the rhizodermis and in the
421 peripheral cortex of bulk-treated seedlings. This could be related to lignification processes as
422 resistance mechanism promoting plant defence (Moura et al., 2010).
423 With histochemical approach, lipid peroxidation was strongly and diffusely detectable in
424 B treated samples, as confirmed by TBARS assay, indicative of membrane damage, mainly in
425 root cortex. In this material the good correlation between TBARS and H_2O_2 content could
426 indicate an H_2O_2-dependent membrane damage. These data are in line with ultrastructural
427 observations on B treated samples. NPs treatments induced, in accordance with biochemical
428 data, a whole signal comparable to the control, apart from a peculiar staining pattern in the
429 outermost layers of vascular cylinder characteristics for the S-NPs. The lack of membrane
430 damage in NPs-treated materials and C roots is in accordance with previous data on *V.*
431 *narbonensis* treated with higher S-NPs concentrations (Ruffini Castiglione et al., 2014).
432 Therefore, *V. faba* root seems to be strongly harmed by bulk material treatment while TiO_2 S-
433 NPs may act inducing a localized tissue-specific membrane damage. To protect cellular
434 structure and metabolism from oxidative damage, plant evolved a complex enzymatic and non
435 enzymatic system. Proline can contribute along with ascorbate and glutathione to ROS
436 detoxification. Given the lower proline content in treated seedlings than in control ones, the
437 main antioxidant roles were played in our conditions by ascorbate and glutathione in
438 accordance with literature (Jiang et al., 2014). The higher pools of both ascorbate and

439 glutathione in bulk-treated material showed the importance of these antioxidants in oxidative
440 stress response. The highest reducing power recorded in NPs-treated roots was in line with the
441 low H_2O_2 content detected in these materials.

442 Enzymatic activities were generally inhibited in treated seedlings, with the exception of
443 GPX characterized by similar activities in all materials. The decrease in CAT activity detected
444 in NPs-treated roots was also relieved in onion seedlings treated with TiO_2-NPs of size similar
445 to that of our P material (Laware and Raskar, 2014) showing the particular sensitivity of this
446 enzyme to TiO_2-NPs. Our results highlighted a different POD activity in dependence from
447 NPs size: in particular the maximum value was observed in S-treated roots, confirming
448 previous data obtained in *V. narbonensis* under different concentrations of the same NPs
449 (Ruffini Castiglione et al., 2014), while in P-NPs roots POD activity was lower than in control
450 roots. These results were basically comparable to those obtained *in situ* by guaiacol-
451 peroxidase staining, resembling the recorded pattern of H_2O_2 staining with a specific
452 involvement of the phloem tissues for the samples treated with both TiO_2-NPs. Guaiacol
453 peroxidase activity, known as having important roles in control of growth by lignification
454 (Gaspar et al., 1991), was stronger in xylem vessels under all the treatments, indicating a
455 precocious status of tracheary element differentiation in respect to the control. This process
456 seems to be more pronounced in the treatments with S-NPs and B material as further
457 confirmed by the localization of RNS, among which NO is involved as signal molecule, in
458 plant cell differentiation, xylogenesis and cell wall lignification (Planchet and Kaiser, 2006).
459

460 **5. Conclusions**

461 On the whole, the low concentration of the different materials was able to induce specific
462 responses in our plant model system. Germination process was stimulated in P-NPs treated
463 seeds. TiO_2, supplied as bulk material, induced oxidative stress, in terms of both H_2O_2 and

TBARS content, disturbance in root growth and in cellular ultrastructure. Genotoxic effects, detectable in bulk treated roots, were however also evident following S-NPs treatment.

In addition *in situ* analysis revealed localized stress signals in specific root compartments related to developmental and/or defence response, typical for the different treatments. In bulk-treated roots antioxidant defence seemed to rely mainly on low molecular weight antioxidants. In the different NPs-treatments a high reducing power of glutathione in P-NPs treated seedlings and a high POD activity in S-NPs treated material were observed. The activation of the antioxidant response in the presence of low levels of H_2O_2 is particularly interesting as it could help to explain the protective action of TiO_2-NPs in plants subjected to abiotic stress. These results all together suggest that TiO_2-NPs, able to penetrate into root cells, may exert different actions depending on their size and their shape and that the bulk counterpart, in our experimental conditions, seems to provoke the major adverse effects in *V. faba* roots.

Acknowledgments

Our special thanks go to Dr C. Vergari and Prof. F. Giammanco (Plasma Tech, Polo Tecnologico Navacchio, Pisa, Italy) for kindly providing P nanoparticles.

This work was supported by local funding of the University of Pisa (ex 60 %).

References

Aebi, H., 1984. Catalase *in vitro*. Meth. Enzym. 105, 121-126.

Arezky, O., Boxus, P., Kevers, C., Gaspar, T., 2001. Changes in peroxidase activity, and level of phenolic compounds during light-induced plantlet regeneration from *Eucalyptus camaldulensis* Dhen. nodes *in vitro*. Plant Growth Regul. 33, 215-219.

Asli, S., Neumann, P.M., 2009. Colloidal suspensions of clay or titanium dioxide nanoparticles can inhibit leaf growth and transpiration via physical effects on root water transport. Plant Cell Environ. 32, 577-584.

Azimi, R., Feizi, H., Khajeh Hosseini, M., 2013. Can bulk and nanosized titanium dioxide particles improve germination features of wheatgrass (*Agropyron desertorum*). Not. Sci. Biol. 5, 325-331.

Baderna, D., Lomazzi, E., Pogliaghi, A., Ciaccia G., Lodi M., Benfenati, E. 2015. Acute phytotoxicity of seven metals alone and in mixture: are Italian soil threshold concentrations suitable for plant protection? Environ. Res. 40, 102–111.

Balestri, M., Ceccarini, A., Forino L.M.C., Zelko, I., Martinka, M.,·Lux, A., Ruffini Castiglione, M., 2014. Cadmium uptake, localization and stress ‑induced morphogenic response in the fern *Pteris vittata*. Planta 239, 1055-1064.

Balestri, M., Bottega, S., Spanò, C., 2014. Response of *Pteris vittata* to different cadmium treatments. Acta Physiol. Plant. 36, 767-775.

Bates, L.S., 1973. Rapid determination of free proline for water-stress studies. Plant Soil 39, 205-207.

Bellani, L.M., Salvini, L., Dell'Aquila, A., Scialabba, A., 2012. Reactive oxygen species release, vitamin E, fatty acid and phytosterol contents of artificially aged radish (*Raphanus sativus* L.) seeds during germination. Acta Physiol. Plant. 34, 1789-1799.

508 Bhawana, P., Fulekar, M.H., 2012. Nanotechnology: remediation technologies to clean up
509 the environmental pollutants. Res. J. Chem. Sci. 2, 90-96.
510 Bradford, M., 1976. A rapid and sensitive method for the quantitation of microgram
511 quantities of protein utilizing the principle of protein-dye binding. Anal. Biochem. 72,
512 248-254.
513 Chichiriccò, G., Poma, A., 2015. Penetration and toxicity of nanomaterials in higher plants.
514 Nanomaterials 5, 851-873.
515 Chuankrerkkul, N., Sangsuk, S., 2008. Current status of nanotechnology consumer
516 products and nano-safety issues. J. Min. Met. Mat. Soc. 18, 75-79.
517 Cotelle, S., Dhyèvre, A., Muller, S., Chenon, P., Manier, N., Pandard, P., Echairi, A.,
518 Silvestre, J., Guiresse, M., Pinelli, E., Giorgetti, L., Barbafieri, M., Engel, F., Radetski,
519 C.M., 2015. Soil genotoxicity assessment-results of an interlaboratory study on the
520 *Vicia* micronucleus assay in the context of ISO standardization. Environ. Sci. Pollut.
521 Res. Int. 22, 988-995.
522 Du, W., Sun, Y., Ji, R., Zhu, J., Wu, J., Guo, H., 2011. TiO_2 and ZnO nanoparticles
523 negatively affect wheat growth and soil enzyme activities in agricultural soil. J.
524 Environ. Monit. 13, 822-828.
525 Feizi, H., Shahram, A., Farzin, A., Saeed, J.P., 2013. Comparative effects of nanosized and
526 bulk titanium dioxide concentrations on medicinal plant *Salvia officinalis* L. Ann. Rev.
527 Res. Biol. 3, 814-824.
528 Frazier, T.P., Burklew, C.E., Zhang, B., 2014. Titanium dioxide nanoparticles affect the
529 growth and microRNA expression of tobacco (*Nicotiana tabacum*). Funct. Integr.
530 Genomics 14, 75-83.
531 Gaspar, T.H., Penel, C., Hagege, D., Greppin, H., 1991. Peroxidases in plant growth,
532 differentiation and development processes, in: Lobarzewski, J., Greppin, H., Penel, C.,

533 Gaspar, T.H. (Eds.), Biochemical, Molecular and physiological aspects of plant
534 peroxidases. Université de Genève, pp. 249-280.
535 Ghosh, M., Bandyopadhyay, M., Mukherjee, A., 2010. Genotoxicity of titanium dioxide
536 (TiO_2) NPs at two trophic levels: plant and human lymphocytes. Chemosphere 81,
537 1253-1262.
538 Giorgetti, E., Muniz Miranda, M., Caporali, S., Canton, P., Marsilia, P., Vergari, C.,
539 Giammanco, F., 2014. TiO_2 nanoparticles obtained by laser ablation in water: Influence
540 of pulse energy and duration on the crystalline phase. J. Alloy Compd. 643, S75-S79.
541 Giorgetti, L., Ruffini Castiglione, M., Bernabini, M., Geri, C., 2011. Nanoparticles effects on
542 growth and differentiation in cell culture of carrot (*Daucus carota* L.). Agrochimica 55,
543 45-53.
544 Giorgetti, L., Ruffini Castiglione, M., 2016. Oil palm *in vitro* regeneration:
545 microdensitometric analysis during reproduction and development. Caryologia, on line
546 first, DOI: 10.1080/00087114.2015.1109953
547 Gossett, D.R., Millhollon, E.P., Lucas, M.C., 1994. Antioxidant response to NaCl stress in
548 salt-tolerant and salt-sensitive cultivars of cotton. Crop Sci. 34, 706-714.
549 Hartley-Whitaker, J., Ainsworth, G., Meharg, A.A., 2001. Copper- and arsenate-induced
550 oxidative stress in *Holcus lanatus* L. clones with differential sensitivity. Plant Cell
551 Environ. 24, 713-722.
552 Hotze, E.M., Phenrat, T., Lowry, G.V., 2010. Nanoparticle aggregation: challenges to
553 understanding transport and reactivity in the environment. J. Environ. Qual. 39, 1909–
554 1924
555 IARC - International Agency for Research on Cancer, 2010. Monographs 93. Titanium
556 Dioxide. http://monographs.iarc.fr/ENG/Monographs/vol93/mono93-7.pdf

557 Jana, S., Choudhuri, M.A., 1982. Glycolate metabolism of three submerged aquatic
558 angiosperm during aging. Aquat. Bot. 12, 345-354.
559 Jiang, H.S, Qiu, X.N., Li, G.B., Li, W., Yin, L.Y., 2014. Silver nanoparticles induced
560 accumulation of reactive oxygen species and alteration of antioxidant systems in the
561 aquatic plant *Spirodela polyrhiza.* Environ. Toxicol. Chem. 33, 1398-1405.
562 Kalyanasundharam, S., Prakash, M.J., 2015. Biosynthesis and characterization of titanium
563 dioxide nanoparticles using *Pithecellobium dulce* and *Lagenaria siceraria* aqueous leaf
564 extract and screening their free radical scavenging and antibacterial properties. Int.
565 Lett. Chem. Phys. Astron. 50, 80-95.
566 Karnovsky, M.J., 1965. A formaldehyde-glutaraldehyde fixative of high osmolality for use
567 in electron microscopy. J. Cell Biol. 27, 137-138.
568 Kaveh, R., Li, Y.S., Ranjbar, S., Tehrani, R., Brueck, C.L., Van Aken, B., 2013. Changes in
569 *Arabidopsis thaliana* gene expression in response to silver nanoparticles and silver ions.
570 Environ. Sci. Technol. 47, 10637-10644.
571 Kim, J.H., Lee, Y., Kim, E.J., Gu, S., Sohn, E.J., Seo, Y.S., An, H.J., Chang, Y.S., 2014.
572 Exposure of iron nanoparticles to *Arabidopsis thaliana* enhances root elongation by
573 triggering cell wall loosening. Environ. Sci. Technol. 48, 3477-3485.
574 Kováčik, J., Babula, P., Hedbavny, J., Švec, P., 2014. Manganese-induced oxidative stress
575 in two ontogenetic stages of chamomile and amelioration by nitric oxide. Plant Sci.
576 215-216, 1-10.
577 Kumari, M., Mukherjee, A., Chandrasekaran, N., 2009. Genotoxicity of silver
578 nanoparticles in *Allium cepa*. Sci. Total Environ. 407, 5243-5246.
579 Kutik, J., Kuthanova, A., Smertenko, A., Fischer, L., Opatrny, Z., 2014. Cadmium-induced
580 cell death in BY-2 cell structure starts with vacuolization of cytoplasm and terminates
581 with necrosis. Physiol. Plant. 151, 423-433.

582 Larue, C., Laurette, J., Herlin-Boime, N., Khodja, H., Fayard, B., Flank, A.M., Brisset, F.,
583 Carriere, M., 2012. Accumulation, translocation and impact of TiO_2 nanoparticles in
584 wheat (*Triticum aestivum* spp.): influence of diameter and crystal phase. Sci. Total
585 Environ. 431, 197-208.
586 Laware, S.L., Raskar, S., 2014. Effect of titanium dioxide nanoparticles on hydrolytic and
587 antioxidant enzymes during seed germination in onion. Int. J. Curr. Microbiol. Appl.
588 Sci. 3, 749-760.
589 Lepeduš, H., Jozić, M., Štolfa, I., Pavičić, N., Hackenbereger, K., Cesar, V., 2005. Changes
590 in peroxidase activity in the peel of Unshiu Mandarin (*Citrus unshiu* Marc.) fruit with
591 different storage treatments. Food Technol. Biotech. 43, 71-77.
592 Liu, W.K., 2011. TiO_2-NPs application in agriculture: a review, in Hendriks, B.P. (Ed.),
593 Agricultural research updates. Nova Publisher, Hauppage, New York, pp. 137-145.
594 Ma, X., Geiser-Lee, J., Deng, Y., Kolmakov, A., 2010. Interactions between engineered
595 nanoparticles (ENPs) and plants: Phytotoxicity, uptake and accumulation. Sci. Total
596 Environ. 408, 3053-3061.
597 Mittler, R., 2002. Oxidative stress, antioxidants and stress tolerance. Trends Plant Sci. 7,
598 405-410.
599 Mohammadi, R., Maali-Amiri, R., Mantri, N.L., 2014. Effect of TiO_2 nanoparticles on
600 oxidative damage and antioxidant defense systems in chickpea seedlings during cold
601 stress. Russ. J. Plant Physiol. 61, 768-775.
602 Moreno-Olivas, F., Gant Jr., V.U., Johnson, K.L., Peralta-Videa, J.R., Gardea-Torresdey,
603 J.L., 2014. Random amplified polymorphic DNA reveals that TiO_2 nanoparticles are
604 genotoxic to *Cucurbita pepo*. J. Zhejiang Univ.-SCI. A 15, 618-623.
605 Moura, J.C.M.S., Bonine, C.A.V., de Oliveira Fernandes Viana, J., Carnier Dornelas, M.,
606 Mazzafera, P., 2010. Abiotic and biotic stresses and changes in the lignin content and

composition in plants. J. Integr. Plant Biol. 52, 360-376.

Nakano, Y., Asada, K., 1981. Hydrogen peroxide is scavenged by ascorbate-specific peroxidase in spinach chloroplasts. Plant Cell Physiol. 22, 867-880.

Navari-Izzo, F., Meneguzzo, S., Loggini, B., Vazzana, C., Sgherri, C.L.M., 1997. The role of the glutathione system during dehydration of *Boea hygroscopica*. Physiol. Plant. 99, 23-30.

Navarro, E., Baun, A., Behra, R., Hartmann, N.B., Filser, J., Miao, A.J., Quigg, A., Santschi, P.H., Sigg, L., 2008. Environmental behavior and ecotoxicity of engineered nanoparticles to algae, plants, and fungi. Ecotoxicology 17, 372-386.

Ortlieb, M., 2010. White giant or white Dwarf? Particle size distribution measurements of TiO_2. GIT Lab. J. Eur. 14, 42-43.

Pakrashi, S., Jain, N., Dalai, S., Jayakumar, J., Chandrasekaran, P.T., Raichur, A.M., Chandrasekaran, N., Mukherjee, A., 2014. *In vivo* genotoxicity assessment of titanium dioxide nanoparticles by *Allium cepa* root tip assay at high exposure concentrations. Plos One 9, e87789.

Parida, A.K., Das, A.B., 2005. Salt tolerance and salinity effects on plants: a review. Ecotox. Environ. Safety 60, 324-349.

Planchet, P., Kaiser, W.M., 2006. Nitric oxide production in plants. Plant. Signal. Behav. 1, 46-51.

Poborilova, Z., Opatrilova, R., Babula, P., 2013. Toxicity of aluminium oxide nanoparticles demonstrated using a BY-2 plant cell suspension culture model. Environ. Exp. Bot. 91, 1-11.

Praetorius, A., Scheringer, M., Hungerbühler, K., 2012. Development of environmental fate models for engineered nanoparticles: a case study of TiO_2 nanoparticles in the Rhine river. Environ. Sci. Technol. 46, 6705-6713.

632 Raliya, R., Biswas, P., Tarafdar, J.C., 2015. TiO_2 nanoparticle biosynthesis and its
633 physiological effect on mung bean (*Vigna radiata* L.). Biotech. Rep. 5, 22-26.
634 Ruffini Castiglione, M., Cremonini, R., 2009. Nanoparticles and higher plants. Caryologia 62,
635 161-165.
636 Ruffini Castiglione, M., Giorgetti, L., Cremonini, R., Bottega, S., Spanò, C., 2014. Impact
637 of TiO_2 nanoparticles on *Vicia narbonensis* L.: potential toxicity effects. Protoplasma
638 251, 1471-1479.
639 Ruffini Castiglione, M., Giorgetti, L., Geri, C., Cremonini, R., 2011. The effects of nano-
640 TiO_2 on seed germination, development and mitosis of root tip cells of *Vicia*
641 *narbonensis* L. and *Zea mays* L. J. Nanopart. Res. 13, 2443-2449.
642 Seeger, E.M., Buan, A., Kästner, M., Trapp, S., 2009. Insignificant acute toxicity of TiO_2
643 NPs to willow trees. J. Soils Sediments 9, 46-53.
644 Sharma, P., Bhatt, D., Zaidi, M.G.H., Saradhi, P.P., Khanna, P.K., Arora, S., 2012. Silver
645 nanoparticle-mediated enhancement in growth and antioxidant status of *Brassica*
646 *juncea*. Appl. Biochem. Biotechnol. 167, 2225-2233.
647 Song, U., Shin, M., Lee, G., Roh, J., Kim, Y., Lee, E.J., 2013. Functional analysis of TiO_2
648 nanoparticle toxicity in three plant species. Biol. Trace Elem. Res. 155, 93-103.
649 Spanò, C., Bottega, S., Lorenzi, R., Grilli, I., 2011. Ageing in embryos from wheat grains
650 stored at different temperatures: oxidative stress and antioxidant response. Funct. Plant
651 Biol. 38, 624-631.
652 Spanò, C., Bruno, M., Bottega, S., 2013. *Calystegia soldanella*: dune versus laboratory
653 plants to highlight key adaptive physiological traits. Acta Physiol. Plant. 35, 1329-
654 1336.

655 Shukla, R.K., Kumar, A., Gurbani, D., Pandey, A.K., Singh, S., Dhawan, A., 2013. TiO_2
656 nanoparticles induce oxidative DNA damage and apoptosis in human liver cells.
657 Nanotoxicology 7, 48-60.
658 USEPA (U.S. Environ Protection Agency), 2010. Emerging contaminants-nanomaterials.
659 http://www.epa.gov/region9/mediacenter/nano-ucla/emerging_contaminant_nanomaterials.pdf
660 Zhao, L., Peng, B., Hernandez-Viezcas, J.A., Rico, C., Sun, Y., Peralta-Videa, J.R., Tang,
661 X., Niu, L., Jin, L., Varela-Ramirez, A., Zhang, J., Gardea-Torresdey, J.L., 2012. Stress
662 response and tolerance of *Zea mays* to CeO_2 nanoparticles: cross talk among H_2O_2, heat
663 shock protein, and lipid peroxidation. ACS Nano 6, 9615-9622.
664 Zheng, L., Hong, F., Lu, S., Liu, C., 2005. Effect of TiO_2-NPs on strength of naturally aged
665 seeds and growth of spinach. Biol Trace Elem Res 104, 83-92.
666

Figure captions

Fig. 1. *V. faba* seedlings. Representative samples after 72h germination in water (control), in the presence of 50mg/L of TiO_2 P-NPs, S-NPs and bulk counterpart (Bulk).

Fig. 2. TEM images of (a) P-NPs (arrows) and (b) S-NPs (arrows). (c) Cell portion of control *V. faba* root. The arrow indicates rough endoplasmic reticulum. (d, e) Cell portions of P-NPs treated roots. The arrows indicate P-NPs. (f) P-NPs in two rhizodermis cell walls (arrows). c, chromatin; m, mitochondria; n, nucleolus; v, vacuole; w, rhizodermis cell wall.

Fig. 3. TEM images of (a) aggregate of NPs (arrows) in the vacuole of S-NPs treated root cell. (b) S-NPs (arrows) in portion of degenerated cytoplasm. The double arrows indicate vesicles with rough membranes; the arrowheads indicate vesicles. (c) Aggregates of S-NPs (arrows) in the rhizodermis cell wall. (d-f) Portions of cells of B treated roots. The arrows indicate smooth endoplasmic reticulum. n, nucleus; dc, degenerated cytoplasm; o, not well recognizable organelles; b, weakly electron opaque bodies; w, rhizodermis cell wall.

Fig. 4. Different behaviour of *V. faba* root apex. Mean values of mitotic index (MI %), aberration index (AI %) and of micronuclei frequency (MNC ‰) recorded after 72h germination in water (control), in the presence of 50mg/L of TiO_2 P-NPs, S-NPs and bulk counterpart (Bulk). Bars represent standard errors. Different letters, within each analyzed parameter, indicate significant differences by Bonferroni's multiple comparison test ($p < 0.05$).

Fig. 5. Representative mitotic abnormalities in TiO_2 S-NPs and Bulk treatments in *V. faba* root tip meristem. (a) Micronuclei; (b-c) sticky chromosomes; (d) laggard chromosome in early anaphase; (e-f) C metaphases; (g) somatic pairing; (h-i) reduction grouping; (j) laggard chromosome in disturbed anaphase; (k-m) chromosome bridges in anaphases.

Fig. 6. Cross hand sections of *V. faba* roots of seedlings after 72h germination in water (control), in the presence of 50mg/L of TiO_2 P-NPs, S-NPs and bulk counterpart (Bulk).
The plate comprehends representative images of *in situ* detection of H_2O_2, of reactive nitrogen species (RNS), lipid peroxidation (Lipid perox) and peroxidase activity (POD activity). Bars indicate 200 µm.

Table 1. Growth and physiological parameters in *Vicia faba* roots of seedlings after 72h of germination in water (control), in the presence of TiO_2 Plasma Tech (P-NPs), Sigma (S-NPs) and bulk counterpart (Bulk). Relative water content (RWC), thiobarbituric acid reactive substances (TBARS), total ascorbate (reduced ascorbate, ASA + dehydroascorbate, DHA), total glutathione (reduced form, GSH + oxidised form, GSSG), ascorbate peroxidase (APX), glutathione peroxidase (GPX), guaiacol peroxidase (POD) and catalase (CAT).

	Control	Bulk	TiO_2 P-NPs	TiO_2 S-NPs
Germination (%)	86.67±4.25a	86.67±2.04a	91.67±3.73a	89.58±2.08a
Root length (mm)	46.62±1.41ab	41.81±1.78b	48.16±1.30a	44.37±1.68ab
Vigour Index	4079.17±76.40b	3696.67±44.10c	4392.59±50.17a	3975.00±28.79b
Water content (%)	94.33±0.13ab	94.77±0.35a	93.13±0.38b	93.70±0.35ab
RWC (%)	89.73±1.04b	94.36±1.80a	84.67±0.52c	88.00±1.76bc
H_2O_2 (µmol g^{-1}DW)	70.06±2.42b	91.43±1.49a	38.95±1.51d	49.21±2.55c
TBARS (nmol g^{-1}DW)	259.34±19.15b	388.38±7.91a	247.54±25.31b	278.83±5.28b
Proline (µmol g^{-1}DW)	78.64±2.14a	53.29±1.54b	44.19±1.63c	38.63±3.67c
Total ascorbate (µmol g^{-1}DW)	108.68±1.08b	128.23±3.01a	97.54±1.33c	106.90±0.37b
ASA/DHA	1.10±0.03c	0.97±0.05c	1.60±0.05b	1.79±0.04a
Total glutathione (µmol g^{-1}DW)	1.22±0.06b	1.43±0.05a	0.97±0.06c	1.09±0.02bc
GSH/GSSG	2.53±0.27b	1.71±0.13b	5.81±0.74a	2.01±0.13b
APX (U g^{-1} protein)	606.60±7.40a	510.27±18.17b	500.63±7.92b	510.80±20.51b
GPX (U g^{-1} protein)	1196.67±11.87a	1037.30±8.45a	1032.57±34.03a	1022.02±67.67a
POD (U g^{-1} protein)	1522.02±38.60c	1647.61±34.12b	1415.27±16.42d	2239.91±20.73a
CAT (U g^{-1} protein)	5049.53±487.63a	3832.88±387.16b	2649.43±131.83b	3031.52±282.09b

Data are the mean of at least three replicates ± SE. Means followed by the same letters within the same row are not significantly different at 1%.

Figure 1

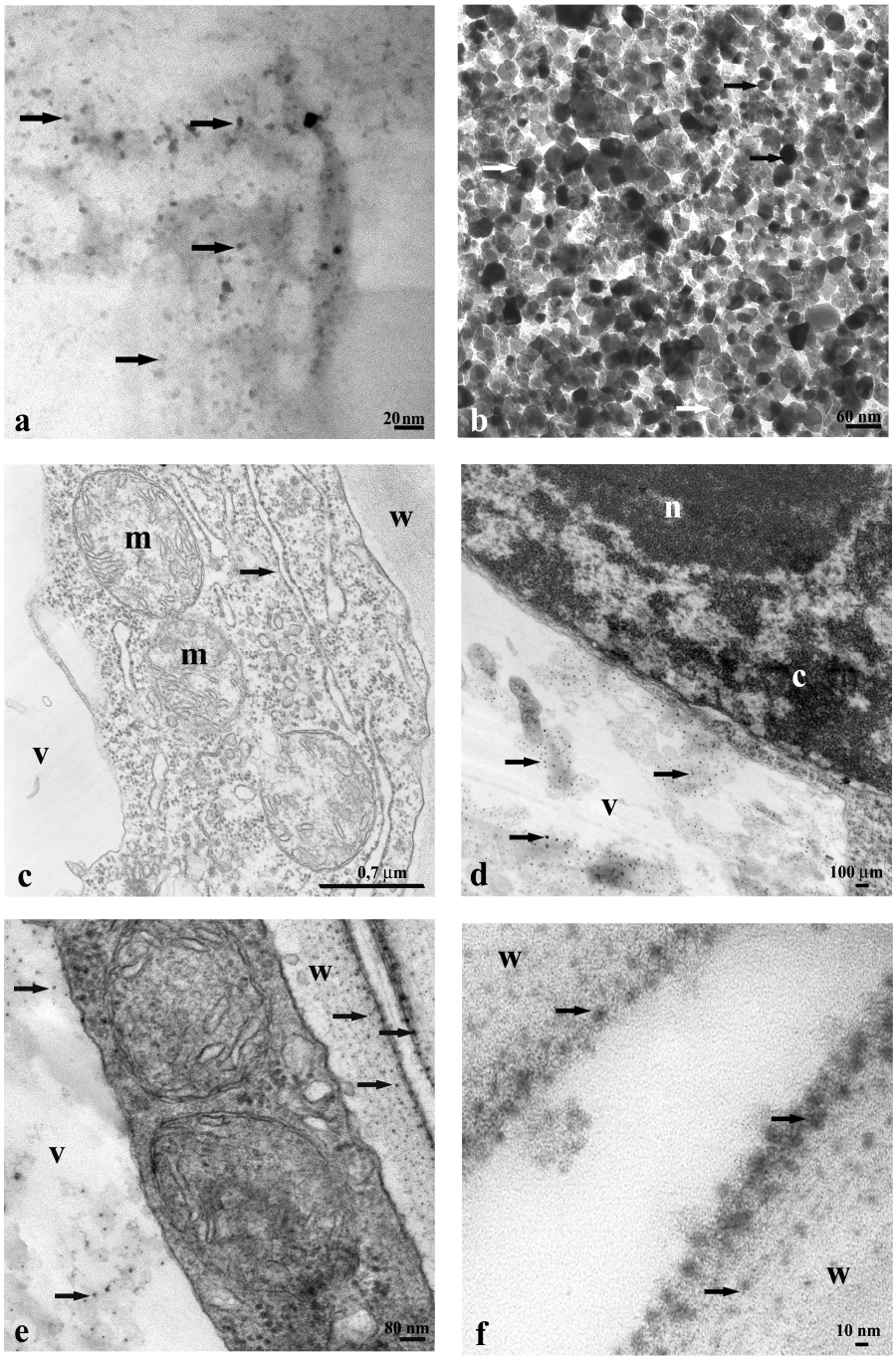

719

720 Figure 2

721

722

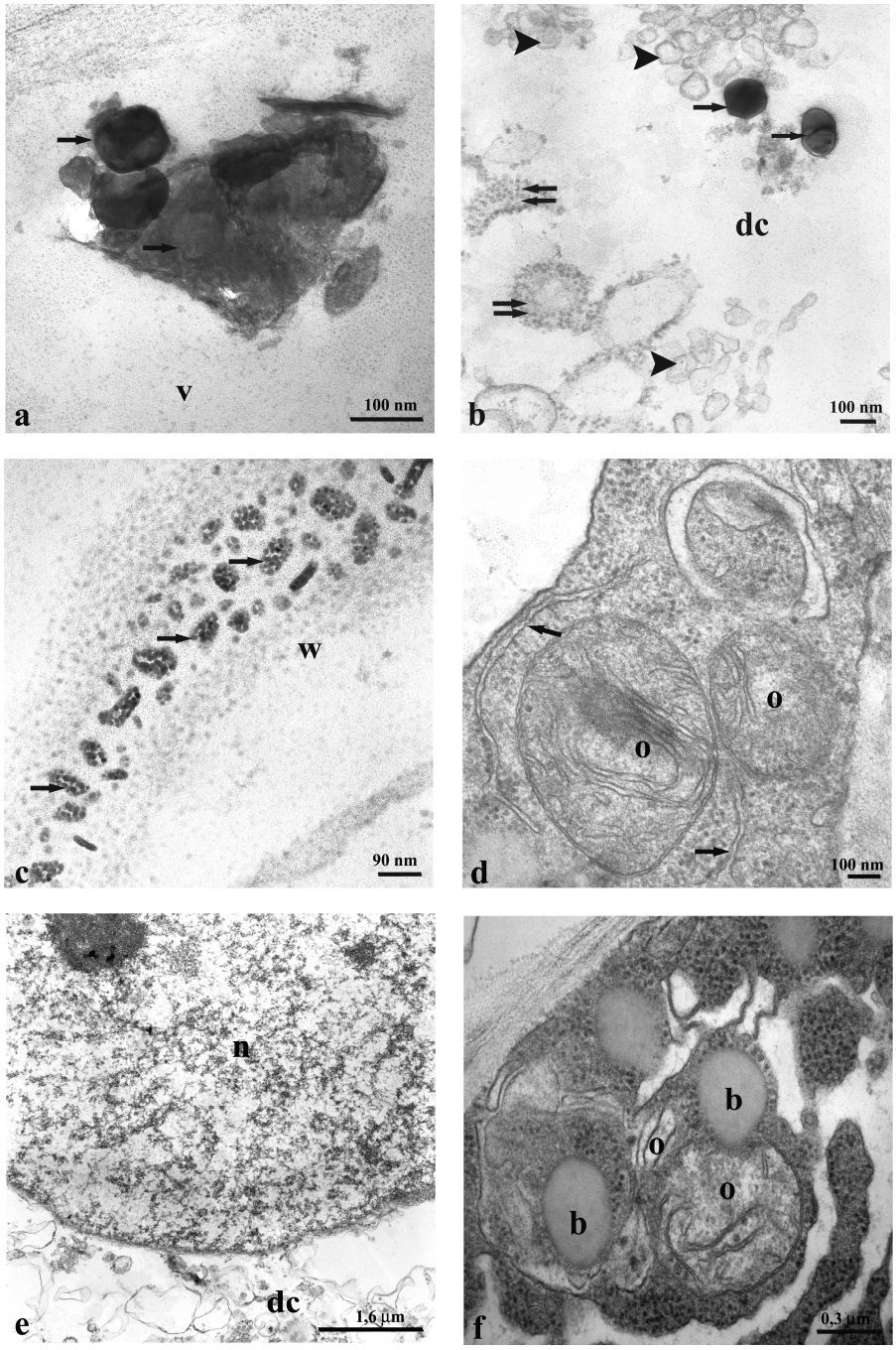

723

724 Figure 3

725

726

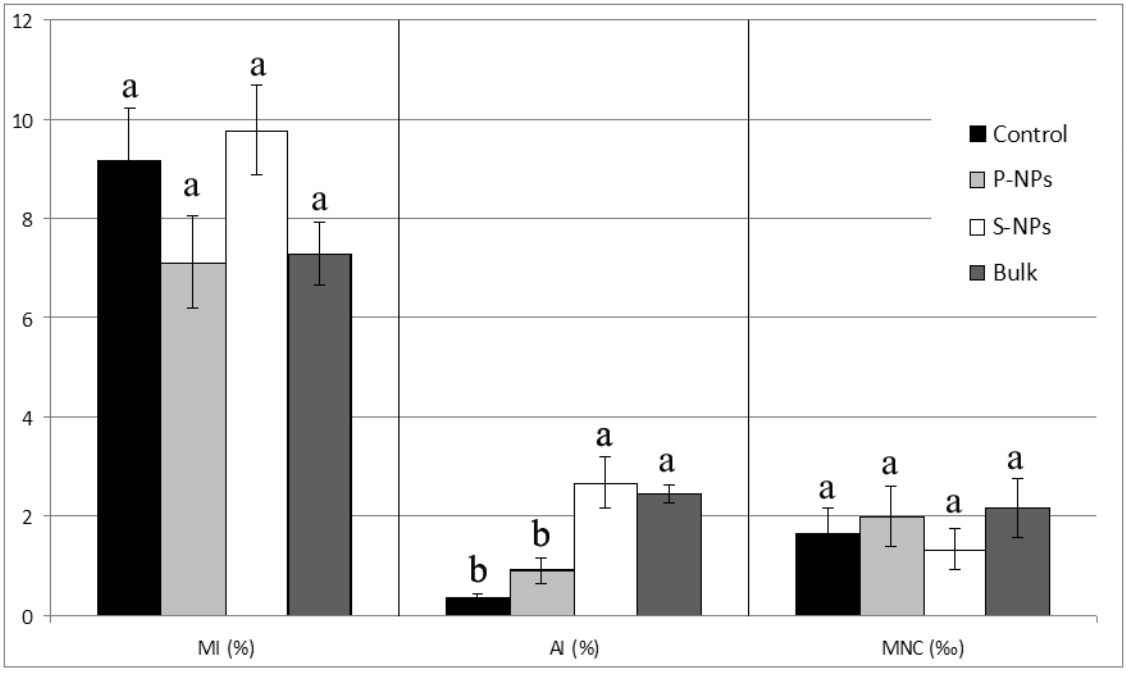

Figure 4

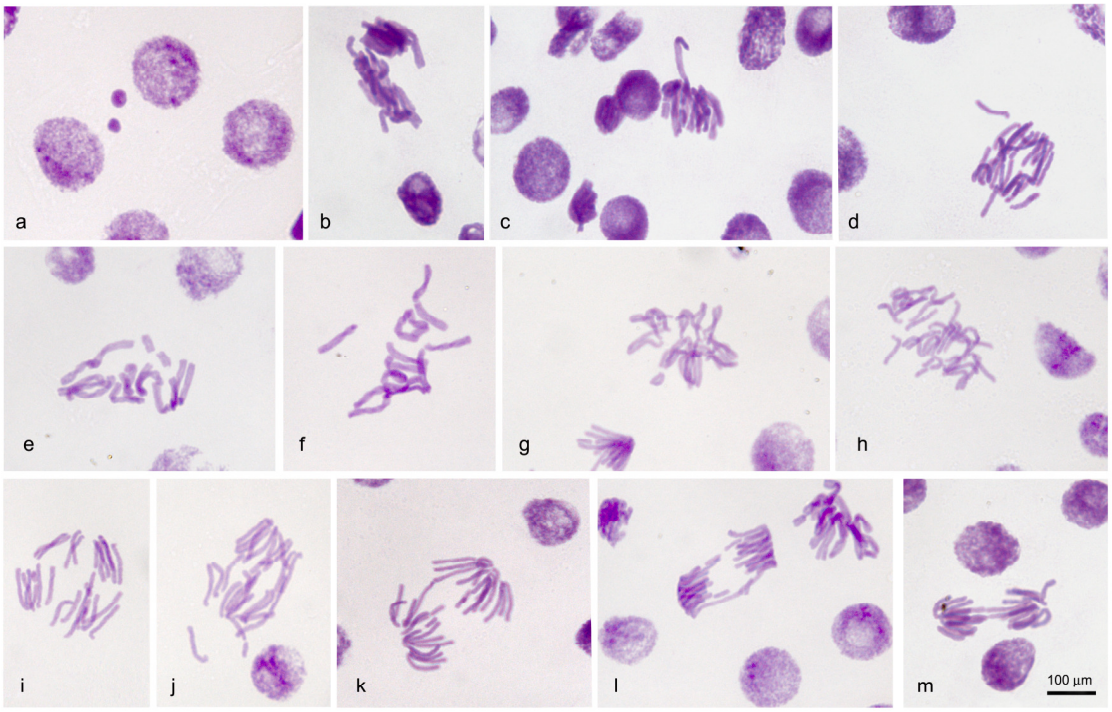

Figure 5

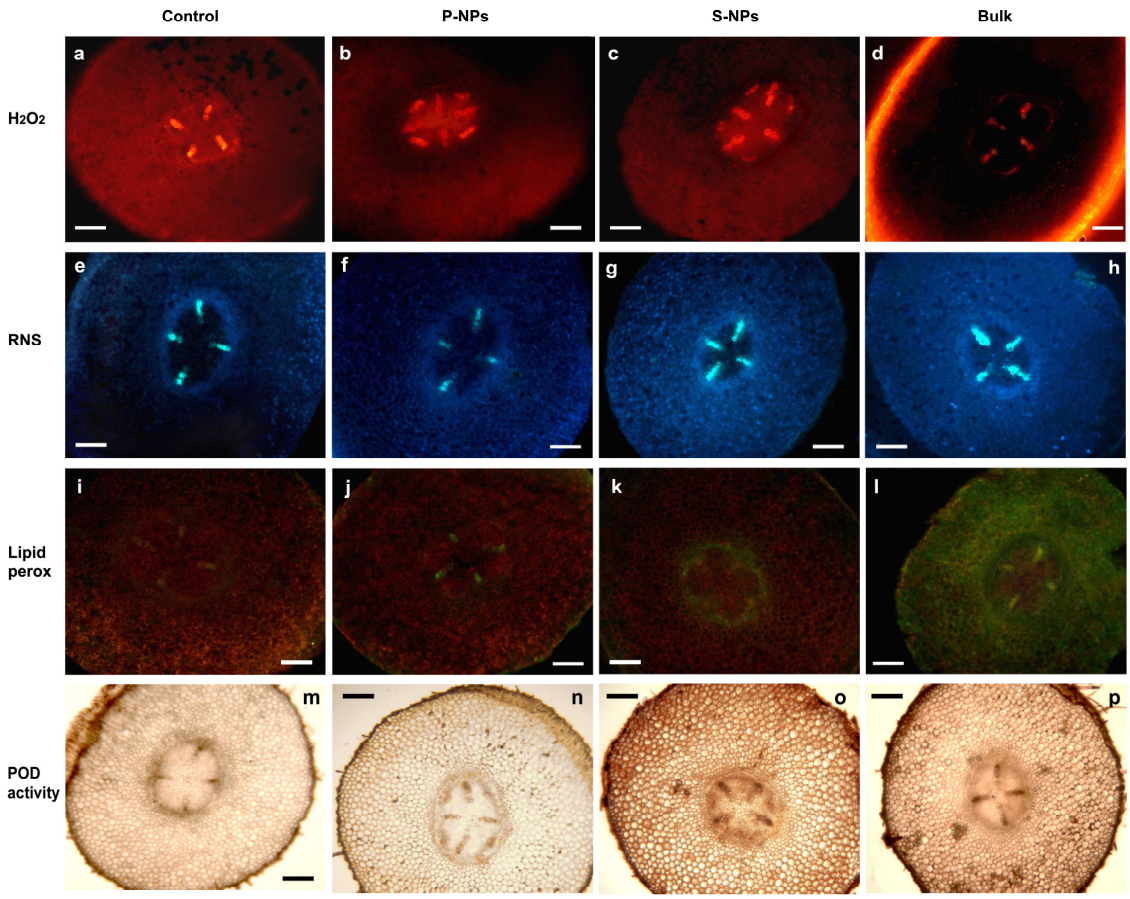
Control
P-NPs
S-NPs
Bulk
H2O2
RNS
Lipid perox
POD activity
a
b
c
d
e
f
g
h
i
j
k
l
m
n
o
p

Figure 6

784
785
786
787
788
789
790
791
792
793
794
795
796
797